

Two complementary approaches for the numerical prediction of meteotsunamis ("rissaga") in Ciutadella harbour (Menorca)

ROMERO, Romualdo; VICH, Mar; RAMIS, Clemente

Grup de Meteorologia, Departament de Física, Universitat de les Illes Balears,

Ctra. de Valldemossa km. 7.5, Palma de Mallorca 07122, SPAIN

romu.romero@uib.es

SUMMARY

The long and narrow inlet of Ciutadella (Menorca, Spain) experiences seiches of about 10.5 min period; during the warm season, these oscillations might reach wave heights around 1 m, and several episodes in its modern history have attained 2-4 m, with catastrophic consequences for the port facilities and moored vessels. The provision of as accurate as possible predictions of this phenomenon, locally known as "rissaga", appears as a crucial element in helping to mitigate these consequences. In this work we devise and inter-compare two different methods.

The first method includes a chain of atmospheric and oceanic numerical simulation components aimed at capturing with relatively low computational cost the key physical processes conducive to most of rissaga events: (i) the genesis and north-eastward propagation of high amplitude atmospheric gravity waves over the Balearic Islands; these waves are synthetically triggered and driven using a 2D nonhydrostatic fully compressible model initialized with the Palma de Mallorca thermodynamic sounding; (ii) the oceanic response along the 80-m deep Menorca channel, in the form of long waves significantly amplified through Proudman-type resonance; (iii) shelf amplification; and (iv) harbour resonance within the 5-m deep inlet of Ciutadella. Second and last steps are modelled according to the shallow-water equations, while the third step owes to Green's law, namely a doubling of the wave amplitude according to the depth jump from 80 to 5 m.

The second method explores the application of a still faster computational approach: a properly trained neural network (NN). In fact, two different NNs are devised and tested: a dry and wet scheme. The difference between schemes resides on the input data, again provided by the Palma sounding; while the first scheme is exclusively focused on the triggering role of atmospheric gravity waves (governed by temperature and wind profiles across the tropospheric column), the second scheme also incorporates the vertical profile of humidity as input information, with the purpose of accounting for the occasional influence of moist convection. We train both NNs using resilient backpropagation with weight backtracking method.

The prognostic systems are successfully tested for the available set of 126 rissaga events and for a complementary set of 549 ordinary situations. Both approaches discriminate fairly well rissaga and non-rissaga situations and are revealed as useful tools for a categorization among weak, moderate or strong cases, even though the NNs tend to underestimate the amplitude of the harbour oscillation. The expected greater versatility of the wet NN over the dry scheme cannot be clearly proved owing to the limited size of the training database.

KEY WORDS

Ciutadella Harbour, Meteotsunami, Rissaga, Atmospheric Gravity Waves, Resonance, Numerical Prediction, Neural networks.

INTRODUCTION

Meteotsunamis are atmospherically induced high-frequency sea level variations (oscillation periods in the range of minutes; Monserrat et al. 2006) that affect many coasts around the world, especially those bays or narrow harbours with high amplification factors, where the local seiches can more easily resonate with the external forcing and develop large amplitudes (Rabinovich, 2009). Given the characteristics of Ciutadella harbour (1.1 km length, 80 m width and 5 m depth) the fundamental period of its seiche is 10.5 min; thus, external forcings with frequencies in the range 5-20 min will be the most effective to lead to a rissaga.

The fundamental atmospheric-oceanic mechanisms leading to rissaga generation were isolated and illustrated by Šepić et al. (2015) (see figure 4 of that paper). First, pressure fluctuations of a few hPa and periods of minutes are generated at sea level due to the tropospheric ducting of high-amplitude internal gravity waves. For these waves to occur, an environment with high wind shear is needed as well as a marked transition from a layer with large static stability (even with a thermal inversion) above the boundary layer, to a mid-tropospheric layer with a steep lapse rate. Given the orientation of the Ciutadella harbour, the required basic current and strong wind shear across the tropospheric column should be preferentially from the W-SW direction. A real example of an optimal combination of atmospheric ingredients is shown in Figure 1, which corresponds to the sounding data taken at Palma de Mallorca station (100 km upstream from Menorca) on 21 June 1984 at 00 UTC. On that day a meteotsunami of 350 cm occurred, the second highest on record.

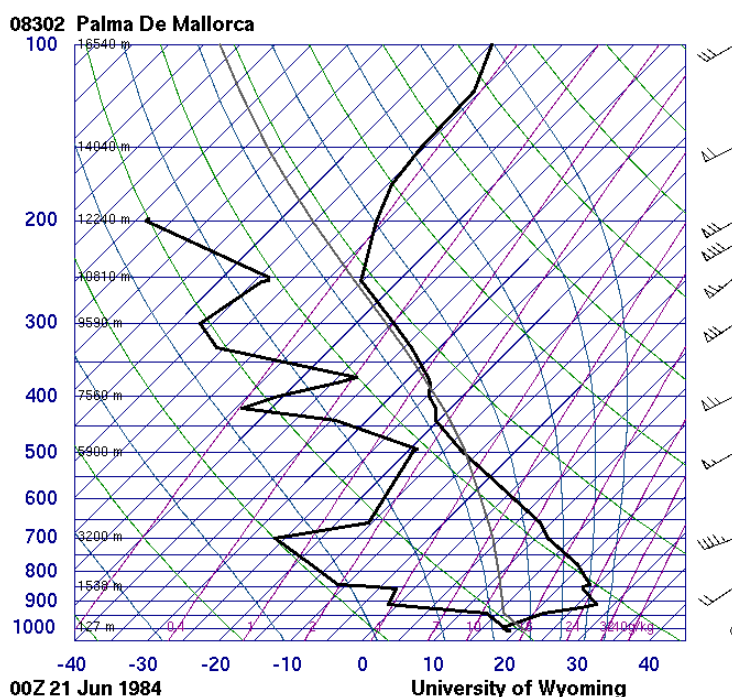


Figure 1: Radio sounding data from Palma de Mallorca on 21 June 1984 at 00 UTC
(source <http://weather.uwyo.edu/upperair/sounding.html>)

In second place, an external forcing provided by long ocean waves travelling north-eastward in the open sea between Mallorca and Menorca (Ramis and Jansà 1983; Marcos et al. 2009) is needed. These waves (with periods predominantly in the range 5-50 min) are driven by the previous atmospheric disturbance, but in order to drive anomalously amplified harbour seiches at Ciutadella they must gain enough amplitude along the ≈ 50 km path separating the islands, before impinging on the mouth of the harbour. The conceptual model by Šepić et al. (2015) emphasizes the Proudman resonance (Proudman, 1929) and shelf amplification (due to shoaling; Green, 1838) as the leading mechanisms for this crucial amplification. Considering the average depth of 80 m of the Mallorca-Menorca channel, the best matching between the long ocean waves and the atmospheric gravity waves will occur when they propagate at speeds of 25-30 m s^{-1} . Additionally, shoaling effects for a depth transition from 80 m in the channel to 5 m of the harbour, would mean doubling the wave amplitude. Together, both mechanisms could increase the ocean wave amplitudes to practically 50-100 cm in most extreme cases before impinging on the Menorca coast.

Finally, Šepić et al. (2015) physical scheme emphasizes the harbour resonance as the last and most evident process for a rissaga generation. That is, the matching of the frequency of incoming long ocean waves and harbour eigenperiods. Of course, periods close to the fundamental mode of 10.5 min will generally be the most effective. Under an optimal sequence of the outlined atmosphere-ocean processes in terms of their attributes (amplitudes, frequencies and propagation speeds), incoming ocean waves can be amplified more than 100 times before hitting Ciutadella coast, entailing a destructive meteotsunami. That was indeed the case on 21 June 1984, as it will be shown later.

Our first approach to build a rissaga forecasting system is based on the direct physical-computational modelling, at relatively low cost, of the above generation mechanisms and their complex interactions (Romero et al. 2019). Since the method uses our own numerical code (called TRAM) we will refer to this first approach as “TRAM-rissaga method”. In essence, for the oceanic phase of the phenomenon, a simple shallow-water model is used to represent the dynamics and amplification of the long ocean waves; for that purpose, we explicitly account for the atmospheric coupling and resonant mechanisms in the equation terms. Regarding the atmospheric domain where all the processes are initiated, our modelling system produces realistic representations of internal gravity waves since we will work at high resolution and use the nonhydrostatic fully compressible equations. To reduce the computational cost of these numerical applications, 2D domains projected over the SW-NE direction are used both in the atmosphere and ocean. In addition, we use flat bottom topographies and initialize the background state of the atmosphere with temperature and wind vertical profiles provided by the representative Palma radio sounding (e.g. Figure 1).

Our second method also links quantitatively the atmospheric ingredients (represented by the wind and temperature profiles) to the wave height recorded at Ciutadella harbour. As artificial neural networks (NNs) are well known algorithms praised for their pattern recognition abilities, we choose such mathematical tools for our objectives. The corresponding method will be referred to as “NN-rissaga method” (Vich and Romero, 2020). In essence, with a properly trained NN we wish to emulate the expert eye of the human forecaster in detecting the risk of rissaga based on the local sounding and synoptic situation of the day, also trying to capture those subtleties of the atmospheric state that can lead to intense cases but which are more elusive to human capacity. It should be noted that once properly trained, a NN is an extremely computationally cheap method, facilitating its future mass application in the operational context.

TRAM-RISSAGA METHOD

The 2D atmospheric model for used for the genesis and propagation of precursor gravity waves, integrates the following equations:

$$\begin{aligned}\frac{\partial \pi'}{\partial t} &= -u \frac{\partial \pi'}{\partial x} - w \frac{\partial \pi'}{\partial z} - w \frac{\partial \bar{\pi}}{\partial z} - \frac{R}{c_v} (\bar{\pi} + \pi') \left[\frac{\partial u}{\partial x} + \frac{\partial w}{\partial z} \right] \\ \frac{\partial \theta'}{\partial t} &= -u \frac{\partial \theta'}{\partial x} - w \frac{\partial \theta'}{\partial z} - w \frac{\partial \bar{\theta}}{\partial z} \\ \frac{\partial u}{\partial t} &= -u \frac{\partial u}{\partial x} - w \frac{\partial u}{\partial z} - c_p (\bar{\theta} + \theta') \frac{\partial \pi'}{\partial x} \\ \frac{\partial w}{\partial t} &= -u \frac{\partial w}{\partial x} - w \frac{\partial w}{\partial z} - c_p (\bar{\theta} + \theta') \frac{\partial \pi'}{\partial z} + g \frac{\theta'}{\bar{\theta}}\end{aligned}$$

where besides the tendencies for the wind in the vertical plane (u , w), predictive equations for Exner pressure and potential temperature perturbations (π' , θ') appear. These perturbations are defined with respect to the sounding-derived horizontally homogeneous reference state (indicated with overbars), a state that is in hydrostatic balance (note that u -velocity component is also initialized using the reference sounding). In addition, the atmosphere is dry and adiabatic and does not include parameterizations of the sub-grid physical processes; all these factors are considered of second order for the problem at hand and can be omitted. The details of the numerical integration scheme of our model, including proper validation tests of its performance, can be found in Romero et al. (2019).

The model runs for a 12h period using a long enough domain of 300 km, where Ciutadella is considered to lie at the central point of this length. The horizontal resolution is $\Delta x=300$ m while in the vertical the domain extends till 20 km height, with Δz progressively increasing from 20 m at sea level to 180 m at the uppermost computational layers. Gravity waves in the simulation are triggered by introducing at the SW boundary a permanent perturbation in the form of a gaussian-shaped vertical profile of downward motion centred at upper-tropospheric levels (see Romero et al. 2019 for details and justification). Only if the environmental characteristics (shear and stability profiles) are supportive of internal gravity waves of high amplitude, mutually adjusted perturbations of the fields (including pressure fluctuations at sea level) will enter the domain and propagate downstream with appreciable magnitude. As an example, Figure 2 shows the simulation obtained with the environment of 21 June 1984. This result highlights the lack of dissipation

of the disturbance as it propagates downstream (from left to right in the figure) and the notable magnitude of the wave near the surface, where it is needed to properly interact with the underlying water body. Additional analyses (not shown here) reveal that the corresponding sea level pressure (SLP) fluctuations possess a significant amplitude, of about 2 hPa, and they propagate across the Mallorca-Menorca channel faster than 20 m s^{-1} , even at $25\text{-}30 \text{ m s}^{-1}$ shortly after 4 h of simulation time, the best scenario for Proudman-type intensification of the forced long ocean waves. A wavelet power spectrum of the SLP wave also proves that most of its energy is focused in periods around 10 min (Romero et al. 2019).

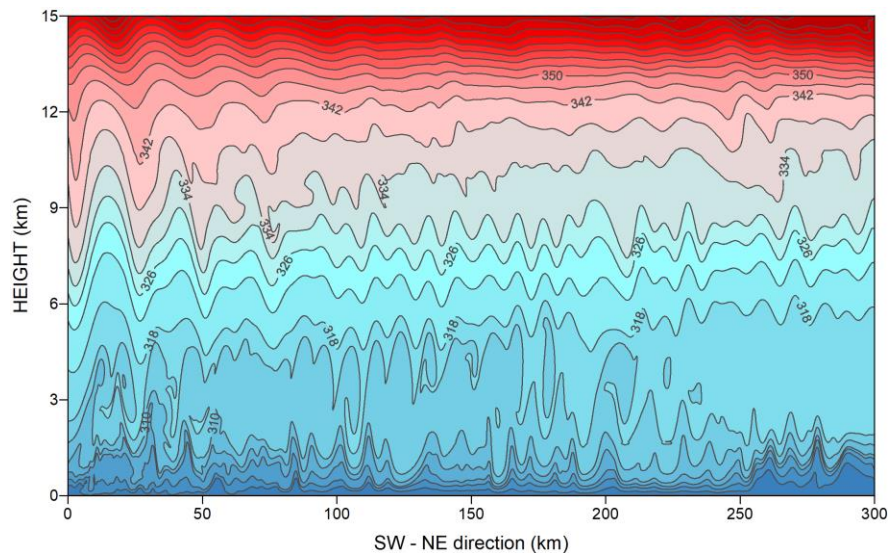


Figure 2. Potential temperature field (contour interval is 4 K) at $t=5 \text{ h}$ corresponding to the atmospheric numerical simulation of the 21 June 1984 case study, that is, using the sounding of Figure 1 for the initialization of the model (source: Romero et al. 2019)

The oceanic response in the Menorca channel is numerically simulated by means of the shallow water equations, after inclusion of the atmospheric forcing term:

$$\frac{\partial h}{\partial t} = -u \frac{\partial h}{\partial x} - h \frac{\partial u}{\partial x}$$

$$\frac{\partial u}{\partial t} = -u \frac{\partial u}{\partial x} - g \frac{\partial h}{\partial x} - \frac{1}{\rho} \frac{\partial P}{\partial x} - \frac{gu^2}{hC^2}$$

In these equations h and u are water depth and velocity, respectively, while P is the space varying sea level pressure provided by the previous atmospheric simulation every 20 s; note we also include a drag force (last term in second equation) following the same formulation of Vilibić (2008). The model is run using a horizontal resolution $\Delta x=600 \text{ m}$ and considering a channel 55-km long, 80-m deep. Non-reflecting boundary conditions are imposed at the SW and NE edges of the domain.

The coastal component of the TRAM-rissaga method runs the same kind of shallow-water model on a domain 1.1 km long and 5 m deep, characteristic of the Ciutadella inlet geometry, using $\Delta x=12 \text{ m}$ but under three fundamental differences: (i) the frictional force is now the only extra term in the momentum equation; (ii) the simulation is forced at the SW boundary, open to the Menorca channel, using the 20-s output of the preceding oceanic simulation, once doubled in amplitude according to Green's law; and (iii) rigid wall conditions are assumed at the NE closed end, where the water depth signal is recorded and scrutinised for possible rissaga oscillations.

Figure 3 shows the specific example of the 21 June 1984 case study. Substantially amplified seiches, owing to the optimal atmosphere-ocean coupling and the action of Proudman and harbour resonances, are obtained at the inlet. The largest of these meteotsunamis is found at around $t=4.5 \text{ h}$ (Figure 3a) with a calculated magnitude (maximum crest-to-trough difference) of 358.3 cm, thus in excellent agreement with the observed magnitude of 350 cm. As expected, the energy of the simulated water depth fluctuations is almost exclusively displayed at periods very close to the fundamental period of the harbour (10.5 min; see Figure 3b).

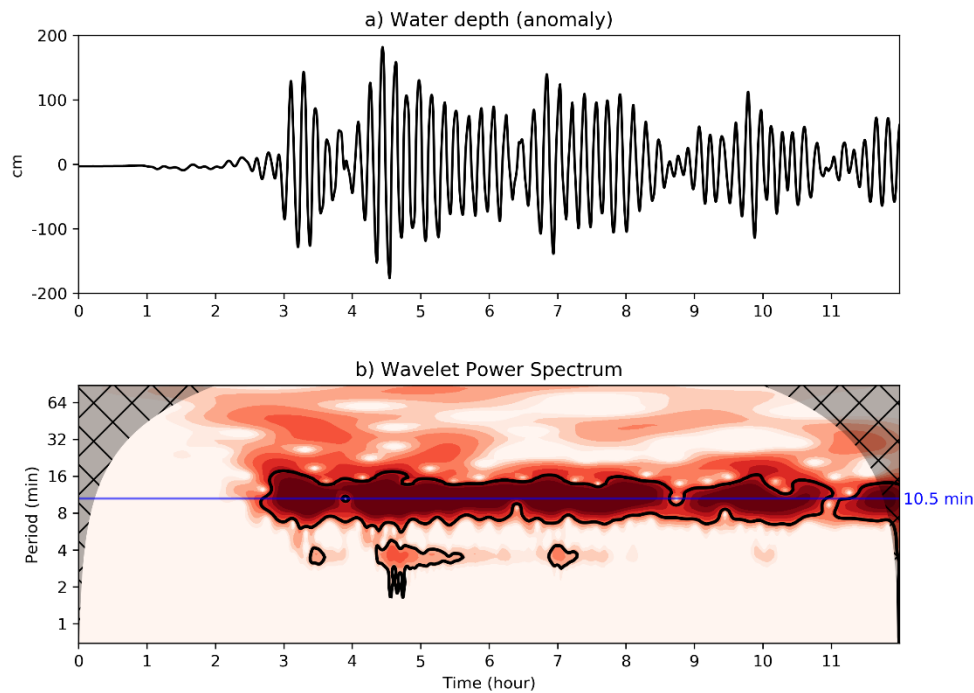


Figure 3. Coastal model simulation of 21 June 1984 case study: (a) Time series of the water depth signal obtained at the end the Ciutadella harbour; (b) Wavelet power spectrum of the water depth series (the indicated period of 10.5 min, in blue, corresponds to the fundamental period of the harbour seiche)
(source: Romero et al. 2019)

NN-RISSAGA METHOD

A neural network is formed by at least three layers: input, output and hidden. The input layer contains the information that is fed to the network. The output layer contains the information we want to predict. Networks can have multiple hidden or middle layers. The hidden layer neurons are governed by an activation function that takes the output of all neurons in the previous layer and delivers a numeric value. This function introduces non-linear properties to the network and therefore increases its versatility. It is crucial to correctly set up these neurons and their connections during the training phase.

Our second rissaga prediction method (Vich and Romero, 2020) uses a recurrent neural network, which is suited to process sequential data aimed at predictions (Schmidhuber, 2015). Specifically, we apply a NN using resilient backpropagation with weight backtracking method (RPROP+, see details in Riedmiller and Rprop, 1994). The R statistics package Neuralnet was used to implement this tool (Fritsch et al., 2019).

The input layer of the NN ingests the sounding-derived environmental features behind rissaga generation: recall, wind direction and vertical shear, and vertical profile of static stability. Specifically, the input layer consists of the Palma radio sounding temperature, u-wind (zonal) and v-wind (meridional) components vertically interpolated to a fixed set of 21 pressure levels, the same set used for the operational outputs of the NCEP/Global Forecasting System (GFS) model. This 63-neuron input layer NN will be referred to as the “dry scheme”. Additionally, we will train a 80-neuron “wet scheme” which also ingests sounding-measured dew point depressions (a measure of the air parcel humidity) throughout the 1000 hPa – 300 hPa atmospheric layer. The motivation for including the humidity profile in this second version of the NN is to take into account the presence of convective or latent instability in the tropospheric column and therefore the chance of convective development. Apart from gravity wave activity, it has been shown that pressure jumps imposed by propagating convective systems would also play a significant role in some rissaga events (e.g. the extraordinary meteotsunamis of 15 June 2006; Jansà et al., 2007).

For the training and validation of the rissaga prediction methods, we were able to compile from different sources a database of 126 rissaga events (i. e. cases with water depth oscillation at the harbour above 70 cm), which extend with notable gaps from July 1981 to July 2018 (plus one old case from September 1975). This population is completed with 549 non-rissaga days (<70 cm) from December 2016 to July 2018 (see Romero et al. 2019 for details). Measured, or at least good estimates, of the maximum water depth

oscillation (crest-to-trough difference) at Ciutadella harbour are available for all these rissaga and non-rissaga days. Both NN schemes have a 1-neuron output layer that corresponds to this measured maximum wave height. They contain 2-hidden layers with a varying number of neurons each. The logistic function was used as activation function.

The whole database, 126 rissaga days plus 549 non-rissaga days, was randomly split into two sets: a training database (70% of the cases) and a validation database (remaining 30%, next section). For each scheme, we choose the best NN configuration based on the following semi-objective criteria on the validation dataset: (1) limited observation-prediction spread; (2) symmetry, i.e. minimally unbiased forecasting; and (3) low degree of overfitting (see Vich and Romero, 2020, for full explanation of these properties).

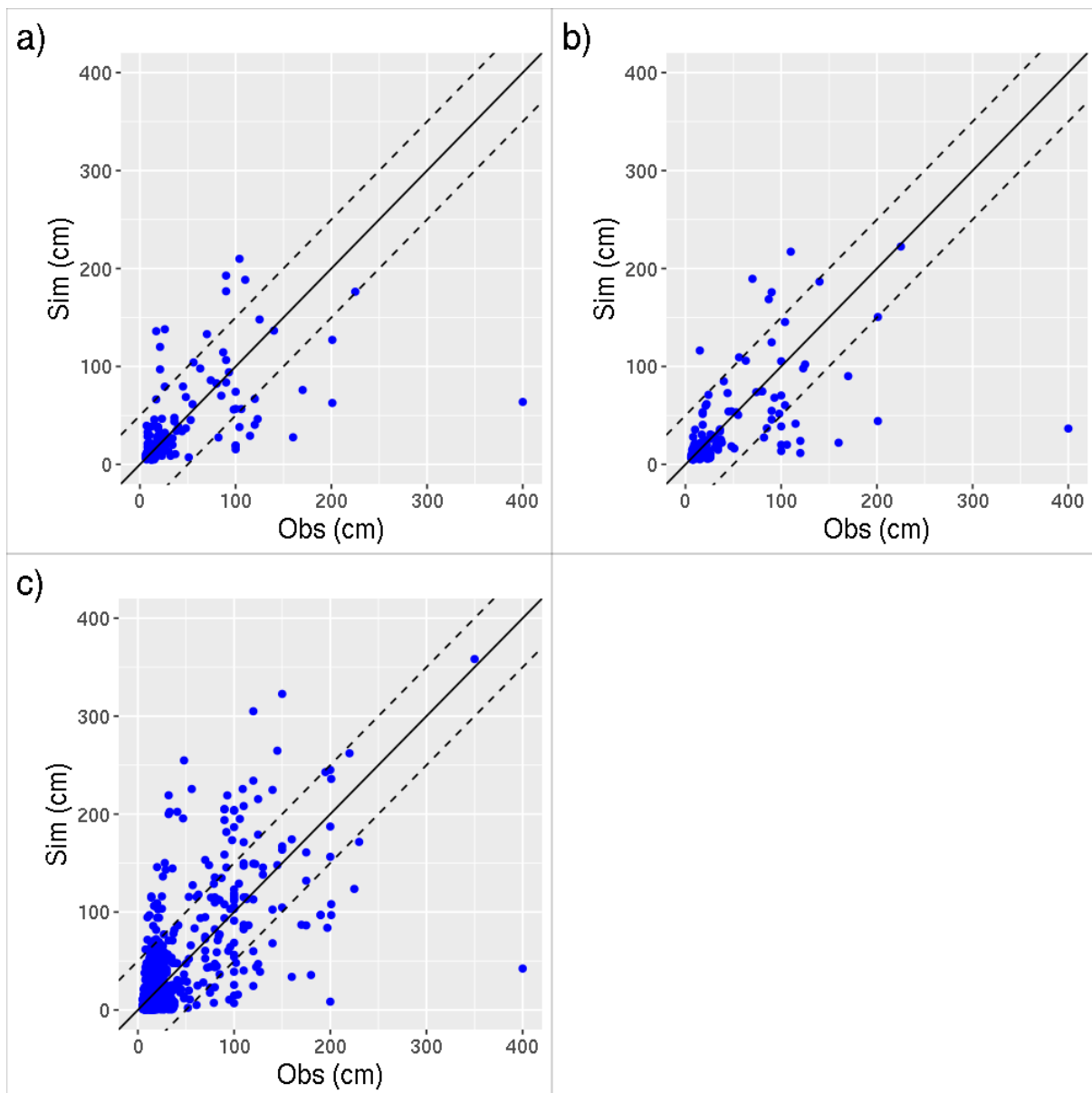


Figure 4. Scatter plots of simulated vs observed water oscillation at Ciutadella harbour obtained by: (a) Dry NN scheme, (b) Wet NN scheme, and (c) TRAM-rissaga method.

Note the last method includes the whole database of events, while the NN schemes only the validation set.

Dashed lines next to the diagonal (solid line) encompass the ± 50 cm limits

(source: Vich and Romero 2020)

PERFORMANCE AND INTER-COMPARISON OF THE RISSAGA PREDICTION METHODS

Considering global results, both NN schemes and the TRAM-rissaga system perform reasonably well (see Figure 4). The difference between observed and simulated mean height at Ciutadella harbour is less than 6 cm for all three systems, although both NN schemes slightly underpredict on average while TRAM-rissaga overpredicts. The root-mean-square error is less than 45 cm for the three systems. Linear correlation coefficients between SIM and OBS in Figure 4 indicate a limited degree of correspondence: correlation coefficient is 0.307, 0.315 and 0.431 for dry, wet and TRAM methods, respectively.

We also computed in Figure 5 five complementary verification scores (see Jolliffe and Stephenson 2012, for a comprehensive guide on forecast verification) considering two different categorization scales of the water depth oscillation: a dichotomous scale, simply distinguishing events from non-events, and an expanded scale based on the intensity of the event (the specific definitions are included in the caption of Figure 5).

The accuracy (ACC, Figure 5a) indicates what fraction of the forecasts are correct. All three methods show good skill in discriminating between non-rissaga and rissaga events. Among the intensity categories, the results for the three rissaga classes (ordinary, intense and extreme) are for all methods outstanding, although the ACC values for the extreme class might be largely influenced by the small number of events that fall into this category.

The bias (BIAS, Figure 5b) indicates whether a predictive system presents a tendency to underforecast (<1) or overforecast (>1) the cases. In this sense, it seems all three methods are well calibrated according to their performance on dichotomous and expanded classes. The results are degraded -and a large spread emerges between TRAM and NN methods- only when considering the poorly sampled extreme rissaga category.

The probability of detection (POD, Figure 5c) indicates the fraction of events that are correctly forecast. The POD value is the highest for the non-rissaga category, more than 90%. The expanded scale categories show a diversity of score values among the forecasting strategies, and there is a clear tendency to lose skill as the magnitude of the oscillation is progressively increased. The spread among the three forecasting techniques also increases from left to right in Figure 5c.

Another well-known verification index is the false alarm ratio (FAR, Figure 5d) which measures the fraction of predicted events that did not occur. As expected, the FAR overall tendency is the opposite of the previous POD behaviour, a common feature of "imperfect" forecasting systems: although all three systems are very well adapted at not generating false alarms for the non-rissaga category, this index increases spread and magnitude as the wave height augments.

Finally, we analyse the probability of false detection (POFD, Figure 5e). This index refers to the fraction of observed non-events that are incorrectly forecast as events. The dichotomous rissaga category and the three rissaga intensity classes show the best (practically perfect) POFD values. POFD is significantly degraded for the weak oscillations, affecting also the spread among techniques.

Overall, and keeping in mind we are facing extreme and physically complex phenomena like meteotsunamis, we find that both rissaga forecasting approaches provide useful results, far from perfect but with reasonable and serviceable skill. According to Figure 5, the physically grounded TRAM method exhibits slightly better scores than the two NN schemes for several indices/categories, but conclusions on its possible superior performance are not robust enough with the data available. The hypothesized improvement of the NN wet scheme over the dry scheme seems rather limited, in part a consequence of the lack of a populated sample of good events for an appropriate training. A remarkable exception is observed for the extreme rissaga category (see Figure 5). This could be expected, since it is precisely for extraordinary events than the roles of deep moist convection and singular surface pressure jumps, have been revealed the most crucial.

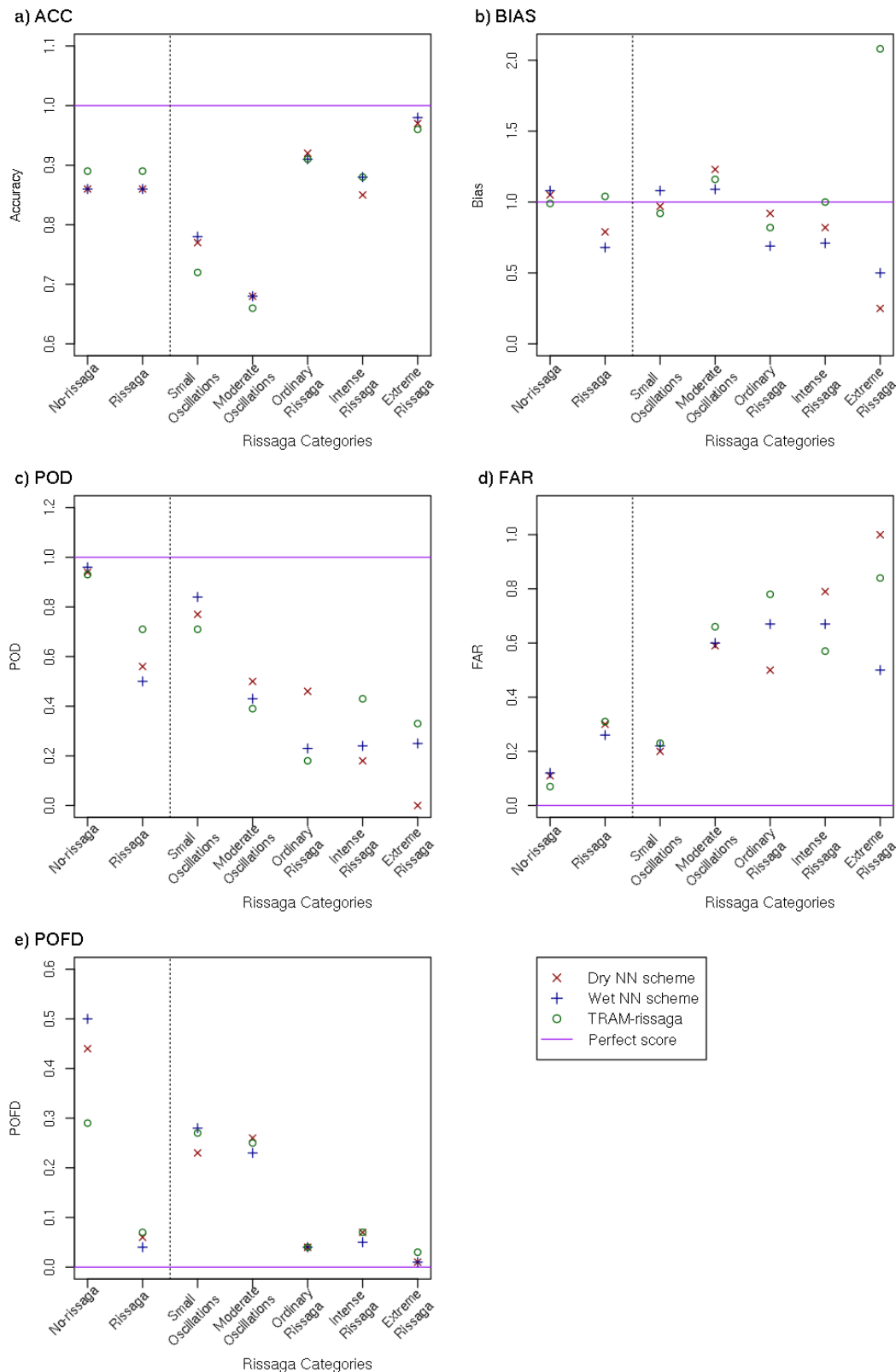


Figure 5. (a) Accuracy, (b) Bias, (c) Probability of Detection, (d) False Alarm Ratio and (e) Probability of False Detection for the three rissaga prediction methods (different symbols according to legend). The purple solid line indicates the perfect score for each corresponding verification index. The following categories are considered: Non-rissaga ($H < 70$ cm) and rissaga ($H \geq 70$ cm) on the left; small (< 20 cm) or moderate oscillations (20-70 cm) and ordinary (70-100 cm), intense (100-200 cm) or extreme (≥ 200 cm) rissaga on the right (source: Vich and Romero 2020)

FINAL COMMENTS AND OPERATIONAL PERSPECTIVE

This study proves that basic knowledge of the leading atmosphere-ocean rissaga generation mechanisms offers very practical tools for predicting Ciutadella meteotsunamis, once this knowledge is translated into simple but physically realistic numerical models (TRAM approach) or into properly trained mathematical algorithms (NN approach). Both schemes showed valuable skill for the recognition of rissaga risk situations and even for their classification as weak, moderate or intense. From beginning to end (i.e. from reading atmospheric sounding data to computation of the maximum sea level oscillation) the TRAM approach merely takes about 5 minutes to run in a standard PC cluster, whereas the application of the NN method takes just a few seconds. The new methods firmly appear as very interesting supplementary approaches to the application of computationally expensive full 3D modelling systems (e.g. the SOCIB/BRIFS system¹, built on the WRF and ROMS models operating at high resolutions and which needs running times of several hours).

With these conclusions in mind, we have implemented operationally both methods for an automatic prediction of rissaga risk and magnitude at Ciutadella harbour. Input data are the pseudo-soundings (vertical profiles of wind, temperature and humidity) extracted from GFS forecasts at the same location of Palma de Mallorca. In addition, fast and sequentially updated wave height predictions are being produced by processing consecutive outputs (e.g. at hourly intervals) of the GFS model. The idea is to combine these lagged predictions into an ensemble forecast of harbour oscillation amplitude, and from these, build probabilistic forecasts of rissaga risk and magnitude. TRAM-derived and NN-derived automatic predictions are publicly available at:

<http://meteo.uib.es/rissaga>

<http://meteo.uib.es/rissaga/NN>

ACKNOWLEDGEMENTS

The development of this work was sponsored by Ministerio de Ciencia e Innovación - Agencia Estatal de Investigación/TRAMPAS (PID2020-113036RB-I00 / AEI / 10.13039/501100011033). We also acknowledge previous contribution by CGL2017-82868-R (COASTEPS) project, an action funded by the Spanish "Ministerio de Economía, Industria y Competitividad" and partially supported with FEDER funds.

REFERENCES

- Fritsch, S., F. Guenther, and M. N. Wright, 2019: Neuralnet: Training of Neural Networks. URL <https://CRAN.R-project.org/package=neuralnet>, r package version 1.44.2.
- Green, G., 1838: On the motion of waves in a variable canal of small depth and width. *Trans. Cambridge Phil. Soc.*, 6, 457-462.
- Jansà, A., S. Monserrat, D. Gomis, 2007: The rissaga of 15 June 2006 in Ciutadella (Menorca), a meteorological tsunami. *Advances in Geosciences* 12, 1-4.
- Jolliffe, I. T., and D. B. Stephenson, 2012: *Forecast verification: a practitioner's guide in atmospheric science*. John Wiley & Sons 380
- Marcos, M., S. Monserrat, R. Medina, A. Orfila, and M. Olabarrieta, 2009: External forcing of meteorological tsunamis at the coast of the Balearic Islands. *Phys. and Chem. of the Earth*, 34, 938-947.
- Monserrat, S., I. Vilibić, and B. Rabinovich, 2006: Meteotsunamis: atmospherically induced destructive ocean waves in the tsunami frequency band. *Nat. Hazards Earth Syst. Sci.*, 6, 1035-1051.

¹ See <http://www.socib.es/index.php?seccion=modelling&facility=rissagaforecast>

Proudman, J., 1929: The effects on the sea of changes in atmospheric pressure. *Geophysical Supplement to the Monthly Notices of the Royal Astronomical Society*, 2(4), 197-209.

Rabinovich, A. B., 2009: Seiches and harbor oscillations. *Handbook of Coastal and Ocean Engineering*, ed. Y. C. Kim (Singapore: World Scientific Publishing Company), 193-236.

Ramis, C., and A. Jansà, 1983: Condiciones meteorológicas simultáneas a la aparición de oscilaciones del nivel del mar de amplitud extraordinaria en el Mediterráneo Occidental. *Rev. de Geofís.*, 39, 35-42.

Riedmiller, M., and I. Rprop, 1994: Rprop description and implementation details. Technical report.

Romero, R., M. Vich, and C. Ramis, 2019: A pragmatic approach for the numerical prediction of meteotsunamis in Ciutadella harbour (Balearic Islands). *Ocean Modelling*, doi 10.1016/j.ocemod.2019.101441.

Schmidhuber, J., 2015: Deep learning in neural networks: An overview. *Neural networks*, 61, 85–117.

Šepić, J., I. Vilibić, A. B., Rabinovich, and S. Monserrat, 2015: Widespread tsunami-like waves of 23-27 June in the Mediterranean and Black Seas generated by high-amplitude atmospheric forcing. *Sci. Rep.*, 5, 11682. doi: 10.1038/srep11682.

Vich, M., and R. Romero, 2020: Forecasting meteotsunamis with neural networks: the case of Ciutadella harbor (Balearic Islands). *Nat. Hazards*, submitted.

Vilibić, I., 2008: Numerical simulations of the Proudman resonance. *Cont. Shelf Res.*, 28, 574-581.